

## Exchange bias effect and large coercivity enhancement in SrRuO<sub>3</sub>/NiO multilayer

This content has been downloaded from IOPscience. Please scroll down to see the full text.

2013 J. Phys. D: Appl. Phys. 46 452001

(<http://iopscience.iop.org/0022-3727/46/45/452001>)

View [the table of contents for this issue](#), or go to the [journal homepage](#) for more

Download details:

IP Address: 210.72.130.48

This content was downloaded on 22/10/2013 at 03:31

Please note that [terms and conditions apply](#).

## FAST TRACK COMMUNICATION

# Exchange bias effect and large coercivity enhancement in SrRuO<sub>3</sub>/NiO multilayer

Xingkun Ning, Zhanjie Wang and Zhidong Zhang

Shenyang National Laboratory for Materials Science, Institute of Metal Research, Chinese Academy of Sciences, 72 Wenhua Road, Shenyang 110016, People's Republic of China

E-mail: [wangzj@imr.ac.cn](mailto:wangzj@imr.ac.cn)

Received 28 July 2013, in final form 19 September 2013

Published 21 October 2013

Online at [stacks.iop.org/JPhysD/46/452001](http://stacks.iop.org/JPhysD/46/452001)**Abstract**

Magnetic multilayers consisting of itinerant ferromagnetic SrRuO<sub>3</sub> (SRO) and antiferromagnetic NiO were pulse-laser deposited on (001) SrTiO<sub>3</sub> substrates. After small-field cooling, enhancements from both the unconventional exchange bias (EB) and the large coercive field were observed in the multilayers. Coercivity values for the in-plane hysteresis loop increased by almost 50 times in comparison with a pure SRO film. The maximum value of the bias moment in the minor loop and the EB field can be achieved in different cooling fields. Moreover, hysteresis indicates a two-step magnetization reversal. We speculate that a pinned layer exists at the SRO/NiO interface producing magnetic regions that pin the ferromagnetic SRO layer.

(Some figures may appear in colour only in the online journal)

Magnetic multilayer structures of 3d- and 4d-series metals have in recent years generated much excitement driven by their potential in both technology and fundamental physics [1, 2]. In multilayer structures comprising different magnetic oxides, such as ruthenate, nickelate and hole-doped manganite, interfacial coupling and charge transfer at the interfaces can lead to various exchange bias (EB) and magnetic effects [3–9]. In strongly correlated transition-metal oxides, perovskite SrRuO<sub>3</sub> (SRO) has been studied intensively because of its interesting magnetic and electronic properties [10]. A substantial amount of work has been devoted to the SRO/La<sub>0.7</sub>Sr<sub>0.3</sub>MnO<sub>3</sub> (FM) and SRO/SrMnO<sub>3</sub> (AFM) multilayers, because these systems feature robust AFM and FM couplings at the interface, making these suitable for studying the different interfacial spin coupling and the interfacial-adjusted magnetic effects [11–13]. Despite extensive studies of the magnetic properties of these periodic structures, however, the valence and spin states of Mn ions are still controversial, making the spin coupling environment at the interface much more complicated [14]. Furthermore, the  $t_{2g}$  ground states associated with FM or AFM are also more important when analysing the interfacial spin interaction in manganites [15].

Nickel oxide (NiO) is a typical 3d transition-metal oxide with a nonmagnetic  $t_{2g}$  state and a rock-salt structure above the Néel temperature ( $T_N = 523$  K) [16]. The  $e_g$ -orbital degrees of freedom are coupled to the lattice distortions at the interface via the exchange-coupling (double exchange or super-exchange) mechanisms [17], which involve the 2p-orbital states at oxygen sites along the Ni–O–Ni bonds. Interestingly, to study the exchange coupling of the SRO/NiO multilayers, one would expect large interfacial coupling because the Ru ions are in high e.g. spin states [18]. Indeed, the Ru 4d states in SRO hybridized more with O 2p states creating larger magnetic moments on the nonmagnetic O atoms [19–20]. The hybridization ( $e_g$ ) of interfacial O 2p with 3d states of Ni ions and 4d states of Ru ions can form FM interactions and thus pin the FM domain of the SRO layers.

In this paper, we report results on the evolution of the EB field and the coercivity with temperature and with the range of magnetic field-cooling of the SRO/NiO multilayer. After field-cooling from room temperature, a distinct EB effect is observed in the SRO/NiO multilayer structure. We have also found that the coercive field ( $H_C$ ) of the SRO/NiO in-plane direction is almost 50 times larger than that of the pure SRO thin film.

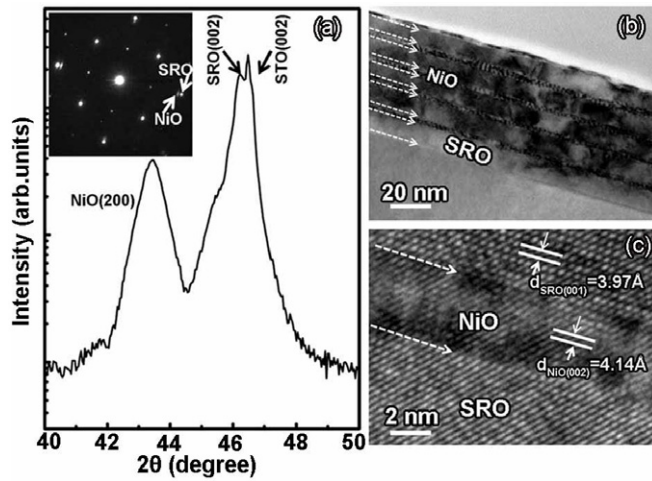


**Figure 1.** (a) XRD spectra of SRO(16 nm)/NiO(4 nm) multilayers. The inset shows the selected-area electron diffraction patterns at the interface region. (b) A low-magnification TEM micrograph of cross-sectional SRO(16 nm)/NiO(4 nm) multilayers. (c) A high-resolution TEM image of SRO/NiO interface region.

SRO/NiO multilayers were grown on single-crystal STO(001) substrates (with a pseudo-cubic lattice and the lattice parameter  $a = 0.391$  nm) by pulsed laser deposition (PLD). The bottom layer SRO (from 2 to 25 nm) is directly grown on the STO substrate followed by the NiO layer (from 0.5 to 25 nm) and then repeated five times. The thickness of SRO and NiO layers was controlled by the deposition time in the PLD process. The films were deposited at 0.5 mbar pressure of pure  $O_2$  at a substrate temperature of 750 °C. The samples were given a final annealing at a pressure of 13 mbar in pure  $O_2$ . For comparison, pure SRO films with the thickness (~75 nm) were also grown on STO substrates under the same conditions.

The x-ray diffraction (XRD) spectra of the SRO/NiO multilayers indicate that the SRO (16 nm) and NiO (4 nm) films are epitaxially grown on the STO(001) substrate (figure 1(a)). Highly (100)-textured SRO films were obtained. Only the (200) peak of NiO can be observed from the XRD data, indicating that the NiO layer is also epitaxially grown on the SRO layer; meanwhile, no secondary phases such as  $Ni_2O$  and  $Ni_2O_3$  exist in the NiO layer. The high-crystalline quality of the multilayers was confirmed by cross-sectional transmission electron microscopy (TEM) images. For example, the interfaces between the SRO and NiO layers are clear and flat with a film thickness of 16 nm and 4 nm, respectively (figure 1(b)). The selected-area electron diffraction patterns of the interface region between the NiO and SRO layers show epitaxial growth of the multilayer (inset of figure 1(a)). A high-resolution TEM image (figure 1(c)) also reveals a clear and well-defined film/film interface (marked by a dashed arrow), in which it is possible to see that both SRO and NiO films have grown epitaxially on the STO substrate.

In-plane magnetic hysteresis loops of the multilayer were obtained at 10 K after field cooling (FC), performed in a magnetic field of 4 kOe from 300 K (above  $T_C$  of SRO but below  $T_N$  of NiO). The absolute values of the EB field  $H_E$ , and of coercivity  $H_C$  are calculated using  $H_E = |H_1 + H_2|/2$

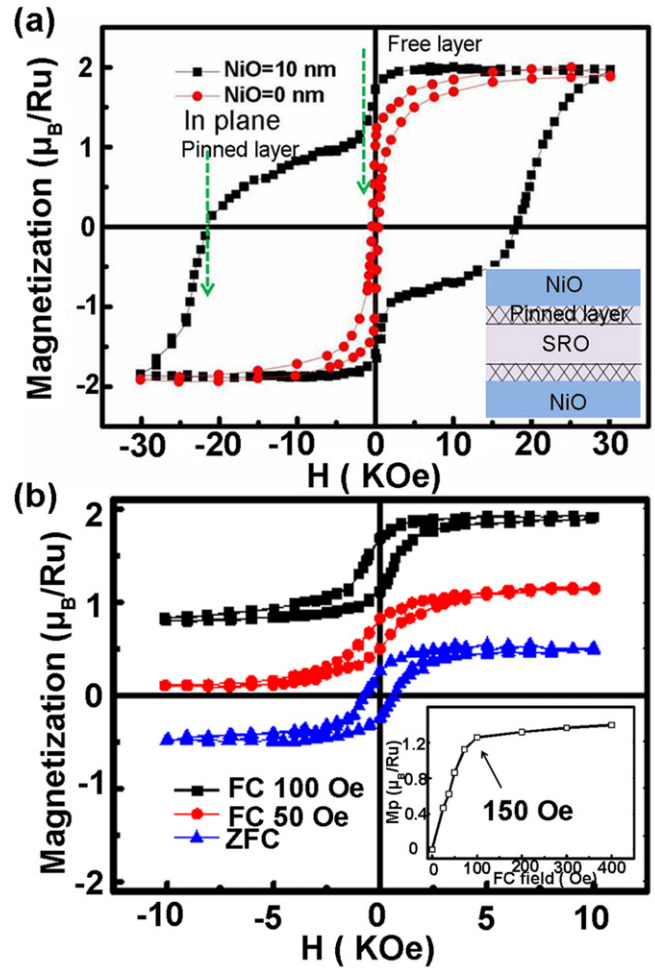


**Figure 2.** (a) Magnetic hysteresis loops of SRO(16 nm)/NiO(4 nm) multilayer and pure SRO film at 10 K after FC. Inset: a schematic picture of the cross section of the interface across the SRO/NiO multilayer. (b) ZFC and FC minor loops of the multilayer at 10 K with magnetic fields of  $\pm 1$  T. Inset: bias moment of the multilayer for different cooling field.

and  $H_C = |H_1 - H_2|/2$ , where  $H_1$  and  $H_2$  are the values of the magnetic field at which magnetization vanishes. For comparison, the magnetization loop for pure SRO film is presented in figure 2(a) and shows that  $H_C$  is about 400 Oe, whereas that of the multilayer with NiO (with total thickness about 20 nm) is about 20 kOe. Similar enhancement in  $H_C$  is also observed for other multilayers with different NiO and SRO thickness. Moreover, the hysteresis loop features a distinctive two-step magnetization reversal (marked by two dashed arrows in figure 2(a)). This phenomenon is similar to the results in the SRO/SrMnO<sub>3</sub> superlattice films [21]. Padhan *et al* have shown that there exists a pinned layer at the interface and Choi *et al* provided direct evidence of the pinned region using x-ray magnetic circular dichroism [13, 22]. Furthermore, the saturation hysteresis loops (sweep from  $-3$  to  $+3$  T) are clearly seen to be shifted along the magnetic-field axis (figure 2(a)), indicating that EB exists in these samples. By analogy, uncompensated spins pinned at the interface indeed exist and should play a similar important role in the interface coupling and the enhanced coercivity of the SRO/NiO multilayer. Thus, the small low-field step in figure 2 arises from the switching of

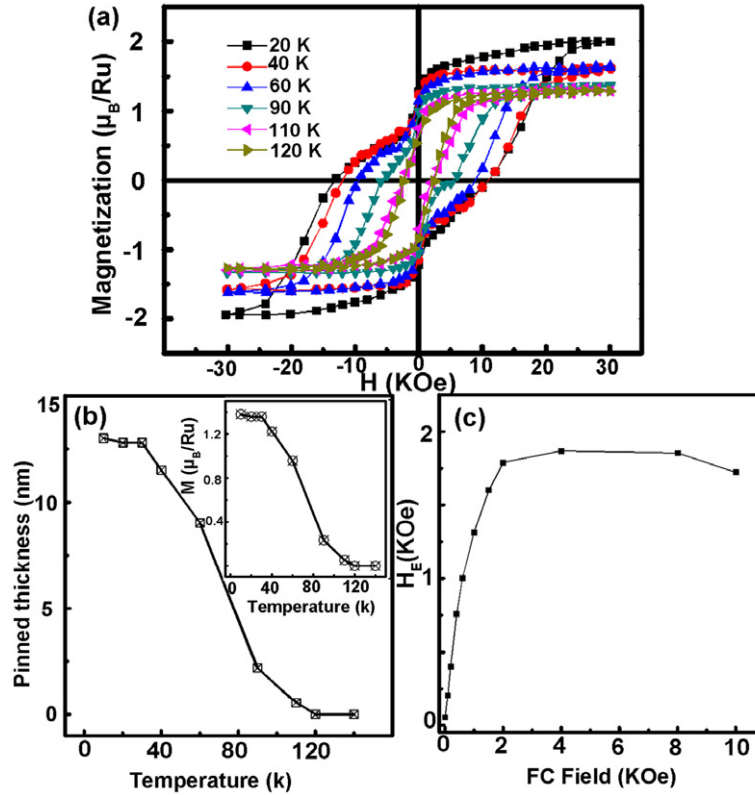


**Figure 3.** (a) Magnetic hysteresis loops of SRO(16 nm)/NiO(4 nm) multilayer at different temperatures after FC. (b) Pinned layer thickness of SRO(16 nm)/NiO(4 nm) versus temperature. Inset: pin moment versus temperature. (c) EB field of the multilayer as a function of cooling field.

free SRO layers and the high-field step can be attributed to the pinned SRO layers at the interface. We also note that the FC minor loop gives a coercivity  $H_C \sim 800$  Oe, which is about two times larger than the pure SRO film ( $H_C \sim 400$  Oe). The results provide evidence that the SRO layers are affected by the interface coupling and can be divided into free layer and pinned interface-layer (see inset in figure 2(a)).

To further understand the switching process underlying the hysteresis loop, several FC minor and saturation loops with different magnetic field ranges have been measured. For example, figure 2(b) shows the zero-field-cooling and FC minor loops, measured in a magnetic field of  $\pm 1$  T, which is smaller than the coercivity of the pinned SRO layer. All the minor loops are symmetric along the field axis. However, the loops are shifted along the magnetization axis and show different bias moments ( $M_P$ ) at different FC fields (see inset of figure 2(b)). The absolute value of  $M_P$  was calculated using relation  $M_P = |M_1 + M_2|/2$  defined by Padhan *et al*, where  $M_1$  and  $M_2$  are the magnetization values at which the magnetic field goes to zero [21]. The  $M_P$  stems from the SRO pinned layer and the minor loop is the magnetization of the free SRO added to this value. The  $M_P$  attains a maximum value at the FC field about 200 Oe, as shown in inset of figure 2(b), which corresponds to a coercivity of the pure SRO films near the Curie temperature. In addition, the two-step magnetization reversal disappeared with the increasing measure temperature, as shown in figure 3(a). We also found that the minor loops are symmetric along the magnetization axis at about 120 K. The Inset of figure 3(b) shows the

absolute value of  $M_P$  obtained from the minor loop (first step) dependent with temperature. What is more, the pin layer thickness  $d$ , as shown in figure 3(b), can be calculated by the saturation magnetization of Ru ( $M_S = 1.7\mu_B$ ) using the pinned model reported by Padhan and Prellier [21]. Interestingly, the thickness of the pinned layer remained constant (about 12 nm) from 10–30 K and then decreased rapidly with increasing temperature and vanished at about 120 K. This established that the pinned effect should have an effective length at low temperature range from the experimental result. It should also be noted that the ferromagnetic domain extended with decreasing temperature, which may related to the pinned layer thickness. After FC from room temperature, the pinned layer formed when the FM domain switched along the applied field at the coercivity of the SRO films. Then the pinned layers increased as the FM domain extended to the inner films of the SRO with decreasing temperature. In addition to this, the uncompensated spin density should increase with increasing FC field and reach a maximum at a higher field. Figure 3(c) shows the  $H_E$  dependence of the FC field for the SRO/NiO multilayer, performed in a magnetic field of  $\pm 3$  T to attain saturated magnetization. It is, indeed, found experimentally that the uncompensated spins pinned at the interface finished at about 2000 Oe. The result is in line with the conventional EB observed in FM/AFM structures [23]. We also measured the  $H_E$  and  $H_C$  of the multilayers with NiO thickness from 0.5 to 20 nm at 10 K (figure 4(a)). The EB is observed even for NiO thickness of only 0.5 nm, reaching nearly saturation at 8 nm. In addition, the coercivity also increases with NiO

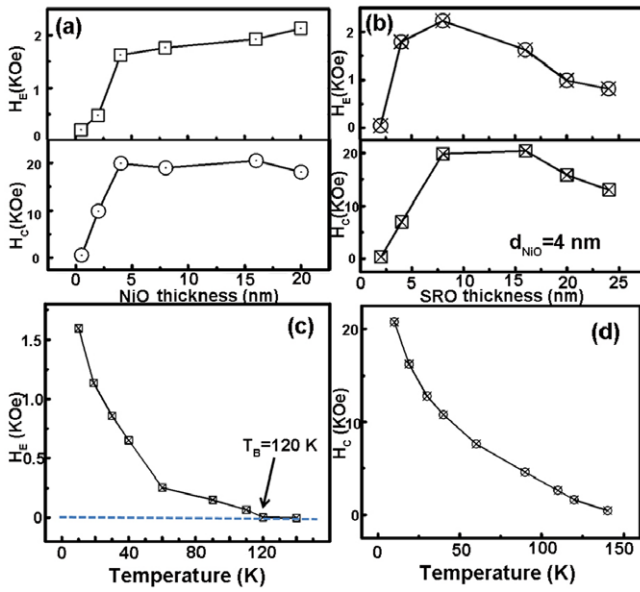


**Figure 4.** EB field  $H_E$  and coercivity  $H_C$  versus NiO thickness (a) and SRO thickness (b). (c) EB field  $H_E$  and (d) coercivity  $H_C$  of SRO/NiO multilayer as a function of temperature (from 10 to 140 K).

thickness which corresponds with the EB field. This may be due to the enhanced in-plane anisotropy energy of the NiO films as the thickness increases. This phenomenon is in line with the conventional EB effect observed in NiCoO/Py and NiFe/FeMn system [24, 25]. But for a given NiO thickness of 4 nm, figure 4(b) shows the dependence of  $H_E$  and  $H_C$  on the SRO thickness.  $H_E$  and  $H_C$  vary in a similar manner, namely,  $H_E$  and  $H_C$  increased first and then decreased with the thickness of SRO. Interestingly, the calculated pinned layer thickness decreases with decreasing SRO layer. The maximum pinned thickness  $d_m$  is about 12.8 nm in the SRO(16 nm)/NiO(4 nm) multilayer. Then the pinned thickness does not change too much with additional increasing of the thickness of SRO films. The coercivity also reached maximum in this pinned thickness. In addition, as has been shown above,  $d_m$  is in correspondence with the temperature data which have been found in the temperature range from 10–30 K; that is to say that the pinned layer may have an effective length. On the other hand, the Fermi level shifted as the itinerant electrons trapped in localized states due to the interface scattering and the epitaxial strain effect. The saturation moment then reduced and the Ni–O–Ru ferromagnetic interaction will be weakened [26]. Our experimental results show that the EB field and coercivity reduced first with the SRO thickness.

Having established this, we now turn to the temperature dependence of the exchange field  $H_E$  and coercivity  $H_C$  of the SRO(16 nm)/NiO(4 nm) multilayer in detail. We measured the hysteresis loops at each temperature after FC from 300 K. Figures 4(c) and (d) show the temperature dependence of the  $H_E$  and  $H_C$  from 10 to 140 K for the SRO/NiO multilayer.  $H_E$  decreases almost monotonically with increasing temperature and vanishes at about 120 K. At the same temperature, the two-step magnetization reversal disappears (figure 3(a)), corresponding to a conventional EB blocking temperature  $T_B$ .

Similarly, from figure 4(d),  $H_C$  also decreases monotonically with increasing temperature. This phenomenon seems to follow the conventional EB effect, which has been observed in FM/AFM structures [27]. Taking into account the above, we speculate that the free and the pinned SRO layers are switched by the same field and the pinned magnetization becomes zero at  $T_B$ . In general, the enhanced in-plane anisotropy derives from the exchange coupling between the SRO and NiO layers. All the experimental results indicate that the 3d Ni and 4d Ru ions indeed strongly interact at the interface. We speculate that the 4d orbitals are more extended than the 3d orbitals; the Ru 4d states are expected to hybridize with the O 2p states and to contribute to the magnetic moment of the O atoms [20]. The two  $Ni^{2+} e_g$  electrons will then show a tendency to interact ferromagnetically through the O atom according to the Anderson exchange theory and the Anderson–Goodenough–Kanamori rule [28, 29]. These results are similar to the result for the FM interaction at  $La_{0.7}Sr_{0.3}MnO_3/NiO$  interface in our previous study [17]. Under these circumstances, one would be expected to calculate the FM coupling strength ( $J_{Ru-Ni}$ ) at the interface and compare with the interaction ( $J_{Ru-Ru}$ ) in the SRO layers. The value of  $J_{Ru-Ni}$  can be estimated using relation  $(J_{Ru-Ni})^2 = 32\pi^2\lambda^{-2}J_{Ru}(t_{SRO})^2M_S H_E$  reported by Padhan *et al*, where  $M_S$  and  $H_E$  are the values of magnetization and EB field. The mean free path  $\lambda = 135 \text{ \AA}$  and  $J_{Ru} \sim 10^{-15} \text{ erg}$  have been used in [21, 30]. We obtain a value of  $J_{Ru-Ni} \sim 10^{-7} \text{ erg}$ , which is much larger than  $J_{Ru} \sim 10^{-15} \text{ erg}$ . The large spin interaction at the interface gives rise to magnetic regions that pin the FM SRO layer and thus form the EB and coercivity enhancement.

In conclusion, we have grown SRO/NiO multilayers and found an EB effect at the interface under the application of an in-plane cooling field. The in-plane coercivity enhancement has interfacial characteristics and arises with the exchange coupling between SRO and NiO layers. Our data provide direct evidence that there indeed exists a large FM interaction across the interface between the Ni and Ru ions. The pinned SRO layers play an important role in its coercivity enhancement.

## Acknowledgments

The partial support of this work by the Hundred Talents Programme of Chinese Academy of Sciences, the National Natural Science of foundation of China (Nos 51072202 and 51172238) and the National Basic Research Programme (No 2010CB934603) of China, Ministry of Science and Technology China is gratefully acknowledged.

## References

- [1] Sharma M, Gazquez J, Varela M, Schmitt J and Leighton C 2011 *Phys. Rev. B* **84** 024417
- [2] Rüegg A, Mitra C, Demkov A A and Fiete G A 2012 *Phys. Rev. B* **85** 245131
- [3] Granada M, Rojas Sanchez J C and Steren L B 2007 *Appl. Phys. Lett.* **91** 072110
- [4] Gilbert M, Zubko P, Scherwitzl R, Iniguez J and Triscone J M 2012 *Nature Mater.* **11** 195

- [5] Zhu S J, Yuan J, Zhu B Y, Zhang F C, Xu B, Cao L X, Qiu X G, Zhao B R and Zhang P X 2007 *Appl. Phys. Lett.* **90** 112502
- [6] Bert J A, Kalisky B, Bell C, Kim M, Hikita Y, Hwang H Y and Moler K A 2011 *Nature Phys.* **7** 767
- [7] May S J, Smith C R, Kim J-W, Karapetrova E, Bhattacharya A and Ryan P J 2011 *Phys. Rev. B* **83** 153411
- [8] Ziese M, Vrejoiu I, Pippel E, Nikulina E and Hesse D 2011 *Appl. Phys. Lett.* **98** 132504
- [9] Ziese M, Vrejoiu I and Hesse D 2010 *Appl. Phys. Lett.* **97** 052504
- [10] Grebinskij S, Masys Š, Mickevičius S, Lisauskas V and Jonauskas V 2013 *Phys. Rev. B* **87** 035106
- [11] Narayana Jammalamadaka S, Vanacken J and Moshchalkov V V 2012 *Europhys. Lett.* **98** 17002
- [12] Ziese M *et al* 2010 *Phys. Rev. Lett.* **104** 167203
- [13] Choi Y, Yoo Y Z, Chmaissem O, Ullah A, Kolesnik S, Kimball C W, Haskel D, Jiang J S and Bader S D 2007 *Appl. Phys. Lett.* **91** 022503
- [14] Choudhury D *et al* 2012 *Phys. Rev. Lett.* **108** 127201
- [15] Hemberger J, Krimmel A, Kurz T, Krug von Nidda H-A, Ivanov V Yu, Mukhin A A, Balbashov A M and Loidl A 2002 *Phys. Rev. B* **66** 094410
- [16] Takahara M, Jinn H, Wakabayashi S, Moriyasu T and Kohmoto T 2012 *Phys. Rev. B* **86** 094301
- [17] Ning X K, Wang Z J, Zhao X G, Shih C W and Zhang Z D 2013 *J. Appl. Phys.* **113** 223903
- [18] Grutter A J, Wong F J, Arenholz E, Vailionis A and Suzuki Y 2012 *Phys. Rev. B* **85** 134429
- [19] Hiraoka N *et al* 2004 *Phys. Rev. B* **70** 054420
- [20] Lee Y B, Caes B and Harmon B N 2008 *J. Alloys Compounds* **450** 1
- [21] Padhan P and Prellier W 2006 *Appl. Phys. Lett.* **88** 263114
- [22] Padhan P and Prellier W 2005 *Phys. Rev. B* **72** 104416
- [23] Wang H, Zhu T, Zhao K, Wang W N, Wang C S, Wang Y J and Zhan W S 2004 *Phys. Rev. B* **70** 092409
- [24] Dimitrov D V, Zhang S F, Xiao J Q, Hadjipanayis G C and Prados C 1998 *Phys. Rev. B* **58** 12090
- [25] Jungblut R, Coehoorn R, Johnson M T, Sauer Ch, van der Zaag P J, Ball A R, Rijks Th G S M, van de Stegge J and Reinders A 1995 *J. Magn. Magn. Mater.* **148** 300
- [26] Xia J, Siemons W, Koster G, Beasley M R and Kapitulnik A 2009 *Phys. Rev. B* **79** 140407
- [27] Prados C, Pina E, Hernando A and Montone A 2002 *J. Phys.: Condens. Matter.* **14** 10063
- [28] Anderson P W 1959 *Phys. Rev.* **115** 2
- [29] Goodenough J B 1955 *Phys. Rev.* **100** 564
- [30] Santi G and Jarlborg T 1997 *J. Phys.: Condens. Matter.* **9** 9563